Toward a better understanding of coagulation for specific extracellular organic matter using polyferric sulfate and polydimethyl diallyl ammonium chloride

Wei Chen[a,b,*], Fengjiao Zhang[a], Huaili Zheng[b], Liangqian Fan[a], Hongbing Luo[a], Yanbo Lu[a], Keqin Feng[a]

[a]*College of Civil Engineering, Sichuan Agricultural University, Chengdu 611830, China, Tel. +86 28 8712772; emails: chenwei0835@163.com (W. Chen), 17784237528@163.com (F.J. Zhang), flqjacky@163.com (L.Q. Fan), luohongbing66@163.com (H.B. Luo), lew619906814@gmail.com (Y.B. Lu), 446283729@qq.com (K.Q. Feng)*
[b]*State Key Laboratory of Coal Mine Disaster Dynamics and Control, Chongqing University, Chongqing 400044, China, Tel. +86 23 65120827; email: zhl@cqu.edu.cn*

ABSTRACT

The impact of extracellular organic matter (EOM) on the coagulation behavior and harvest of algae remains unclear. In this study, bounded EOM (bEOM) and dissolved EOM (dEOM) extracted from laboratory-grown *Microcystis aeruginosa* were characterized in terms of specific ultraviolet absorbance, molecular weight (MW) distribution, Three dimensional excitation emission spectrum (3D-EEM), and component content. Three coagulants, namely, polyferric sulfate (PFS), polydimethyl diallyl ammonium chloride (PD), and PFS-PD, were used to determine the suitable coagulant and conditions for EOM removal. The coagulation behavior for EOM removal and the roles of EOM on algae water treatment were investigated. Results indicated that PFS-PD exhibited the highest efficiency in removing dissolved organic carbon. MW distribution and 3D-EEM analysis showed that the removal of high-MW protein-like substances in bEOM was acceptable and few low-MW microbial product-like and fulvic/humic-like substances in dEOM were coagulated. In addition to charge neutralization, the complex interaction mechanisms between N–H/C–N groups of bEOM and hydroxyl iron facilitated the formation of primary microflocs. High-MW fraction in bEOM promoted floc growth and sedimentation. EOM contributed to the removal of algae cells with its adherence to the surface of cell wall, and no positive impact was observed for the dissociative EOM.

Keywords: Algae; Dissolved extracellular organic matter; Polyferric sulfate; Coagulation mechanism

1. Introduction

The increase of phytoplankton, especially the algae population in surface waters as a consequence of eutrophication of aquatic environments, has become a serious environmental issue that significantly threatens water quality and safety. When seasonal algae bloom and algae cell reproduction becomes excessive, algae organic matter (AOM) derived from algae metabolic activity and released through cell lysis during growth and decline comprises an essential component of natural organic matter in the source water supplying drinking water treatment facilities [1–3]. AOM, which is discovered in most algae, such as *Chlorella*, *Microcystis aeruginosa*, and *Scenedesmus*, covers a wide spectrum of chemical constituents, including carbohydrates (e.g., saccharides, polysaccharides, starch) [4–6], organic acids (e.g., glycolic acid, lipids and fatty acids) [7], and nitrogen-containing

* Corresponding author.

compounds (e.g., nucleic acids, amino acids, and proteins) [4,8]. AOM on an intact cell is normally classified into intracellular, cellular, and extracellular organic matter (EOM) depending on its location in the cells [9]. EOM in source water can cause unpleasant taste, odor compounds, and toxic metabolites and form disinfection by-products during drinking water chlorination [3,6].

EOM extracted from algae is further defined as bounded EOM (bEOM), which adheres to the cell wall, and dissolved EOM (dEOM), which is released in the culture medium [8]. Previous literature indicated that the dominant bEOM constituents are peptide/protein and polysaccharide compounds, with peptide/protein, polysaccharide, and humic substances forming a large proportion of dEOM [6,8]. Although the composition and characteristics of bEOM and dEOM are strongly dependent on the species, growth phase, and culture conditions, the organics with high molecular weight (MW) and strong hydrophobicity comprise a large proportion of bEOM, and the fractions with low-MW and hydrophilicity account for a large proportion of dEOM [4,9]. Conventional water treatments involve membrane filtration [3,6,10], activated carbon adsorption [11], and coagulation [9,12,13]. bEOM and dEOM may substantially affect the water treatment efficiency. During membrane treatment, low-MW organics of dEOM go deep into the internal pore structure of the fiber membrane, and the hydrophobic fraction of bEOM adheres to the membrane surface and forms a dense cake layer, resulting in the increase of irreversible membrane fouling and decrease of membrane flux [10,14]. On the contrary, Henderson suggested that protein-like compounds with high-MW act as a polymer aid with satisfactory removal efficiency [15]. Although considerable attention has been paid to EOM removal by various technologies, few studies have investigated the coagulation of bEOM and dEOM. The selection of a suitable coagulant, variation of major components (e.g., constituent, MW, content), roles of bEOM and dEOM, and dominant mechanisms during coagulation is starving for exploring.

This study aimed to provide deep insight into the coagulation behavior of bEOM and dEOM. Here *M. aeruginosa* was used as the candidate species because it is commonly found in fresh water bloom. bEOM and dEOM were stripped and extracted through frozen centrifugation, and the optimal coagulant and coagulation conditions for bEOM and dEOM removal were optimized. To better assess the coagulation behavior, the specific ultraviolet absorbance (SUVA), main compounds (e.g., dissolved organic carbon (DOC), proteins, and polysaccharides), MW, and three dimensional excitation emission spectrum (3D-EEM) of organics were analyzed. The interactions of EOM and coagulants were evaluated through zeta potential, Fourier-transform infrared spectroscopy (FTIR), and floc size distribution.

2. Materials and methods

2.1. Algae culture and EOM extraction

Laboratory-cultured *M. aeruginosa* was obtained from the Institute of Hydrobiology, Chinese Academy of Sciences, China. Algae culture was conducted in batch mode in a 1 L conical flask with BG11 medium at 25°C, 5,000 lx illumination and 14 h light/10 h dark cycle [16]. The major ingredients

of the BG11 medium are listed in Table 1. The growth and concentrations of *M. aeruginosa* were monitored by counting the cell quantity based on the absorbance at 680 nm wavelength [9,17].

EOM was extracted from algae culture media in the phases on the 16th day (stationary phase), in which the concentration was approximately 6.50×10^8 cells L^{-1}. The extraction of bEOM and dEOM from algae medium was performed using a high-speed versatile refrigerated centrifuge (3-18R, Hengnuo, China) at 10,000 and 4,000 g, respectively [4,8]. Specifically, the algae medium was first centrifuged at 4,000 g for 15 min. The supernatant in the centrifuge tube was filtered through a 0.45 μm microfiltration membrane, and the filtrate solution was referred to as dEOM. Subsequently, the algae cells (on the membrane surface and at the bottom of the centrifuge tube) were collected and resuspended in the same volume of 0.6% NaCl solution. The resuspended cell solution was recentrifuged at 10,000 g for 15 min before filtering, and the obtained filtrated solution was referred to as bEOM. The extracted bEOM and dEOM solutions were stored in a refrigerator at 4°C and analyzed within 72 h.

2.2. Characterization and analysis of bEOM and dEOM

DOC was determined with a total organic carbon analyzer (Elementar, Germany). Protein content analysis was performed using a modified Lowry method, with a bicinchoninic acid protein assay kit acquired from Shanghai Rebus Network Technology Co. Ltd. (Shanghai), and a UV/Vis spectrophotometer (UV-4802S, UNICO, USA) at 562 nm wavelength nm was calibrated with bovine serum albumin [8]. Phenol sulfuric method was adopted to determine the polysaccharide concentration [18]. UV_{254} was measured using a spectrophotometer, and the SUVA of EOM was calculated as SUVA $(m^{-1} mg^{-1} L) = UV_{254}(cm^{-1})/DOC(mg/L) \times 100$. ζ-potential of the solution was obtained with a Zetasizer Nano ZS90 (Malvern, UK). All analyses were repeated thrice, and their reproducibility was acceptable with a deviation less than 5%.

Ultrafiltration (UF) fractionation was adopted to distinguish the MW distributions of EOM fractions. Specifically, the EOM suspension in a 300 mL cup-type filtration vessel was driven by 0.1 MPa nitrogen gas through a series of

Table 1
Ingredients of BG-11 medium

Ingredient	Concentration (g L^{-1})
NaNO3	1.5
K_2HPO_4	4.0×10^{-2}
$CaCl_2 \cdot 2H_2O$	3.6×10^{-2}
Citric acid	6.0×10^{-3}
Ammonium ferric citrate	6.0×10^{-3}
Sodium ethylenediaminetetraacetate (EDTANa$_2$)	1.0×10^{-3}
Na_2CO_3	0.02
$MgSO_4 \cdot 7H_2O$	7.5×10^{-2}
Soil suspension	–

regenerated polyethersulfone UF membranes (Pall, USA) with MWs of 100, 30, 10, and 1 kDa, resulting in EOM fractions of >100, 30–100, 10–30, 1–10, and <1 kDa. Ultrapure water (2,000 mL) water was filtrated before UF fractionation. Stirring at 150 rpm was performed to prevent the formation of a cake layer and reduce the concentration polarization. The organic matters in each fraction were measured in terms of DOC, protein, and polysaccharide.

3D-EEM was applied to analyze the change of certain classes of organic matter before and after coagulation. To accurately evaluate the difference of major components between bEOM and dEOM, dEOM was diluted with boiled water at the same DOC concentration as that for bEOM. The 3D-EEM fluorescence of the bEOM and dEOM solutions were scanned and recorded in cells with a 1.0 cm path length using a Hitachi F-7000 fluorescence spectrometer (Tokyo, Japan) with a 700 V xenon lamp at room temperature (20°C ± 2°C). The emission spectra were recorded from 200 to 500 nm at 2 nm increment, and the excitation spectra were measured from 200 to 400 nm at 5 nm increment. Subsequently, the collected data were processed and plotted on Origin 8.5.

2.3. Coagulation experiment

Three coagulants, namely, polyferric sulfate (PFS, basicity: 11.5% ± 0.1%, laboratory-prepared based on the literature of Chen et al. [19]), polydimethyl diallyl ammonium chloride (PDMDAAC (PD), intrinsic viscosity: 3.3 ± 0.1 dL/g, commercially purchased from Yiwu Xinbang Environmental Protection Technology Co. Ltd. (Zhejiang, China)), and composite coagulant PFS-PD (PFS: PDMDAAC = 10:1, laboratory-prepared through mixing diluted PFS and PDMDAAC solution), were adopted in beaker test. PFS and PDMDAAC were diluted in 10 and 2 g L^{-1} distilled water, respectively. Table 2 displays the water quality parameters of bEOM and dEOM solutions. Coagulation jar experiments were conducted using a programmable jar test apparatus with six 500 ml glass beakers (ZR4-6, Shenzhen Zhongrun Water Industry Technology and Development Co. Ltd., China) at room temperature. After the addition of a specific amount of coagulant in the water sample, high-speed (250 rpm) and low-speed (30 rpm) coagulation at 1 and 10 min were conducted, respectively, followed by 30 min settling. The supernatant sample was extracted from the beakers with a syringe 1 cm below the water surface and filtered through a 0.45 μm membranes filter for subsequent testing. The

zeta potential of colloidal particle was determined with the completion of the rapid mixing phase.

To evaluate the roles of bEOM and dEOM on the harvest of algae cells, five types of algae solutions were prepared and coagulated. The details of the algae solutions in flocculation experiments are listed in Table 3. Owing to that the algae cells are unevenly distributed in the supernatant, the harvest efficiency was represented in terms of chlorophyll-a (Chl-a) removal rate. Chl-a concentration was determined based on Chinese national standards (No. SL88-2012) in the test [20].

2.4. Floc characterization

After coagulation, the flocs at the bottom of the beaker were systematically collected, and the floc size distribution was determined with a Mastersizer 2000 laser diffraction instrument (Malvern, UK) at a slow stirring agitation of 30 rpm to keep the aggregates suspended. Before the structure and morphology measurement, the flocs were dried in a vacuum dryer and ground with a laboratory mortar and pestle. The floc powder was sampled with potassium bromide, and FTIR characteristic peaks at 4,000–400 cm^{-1} were obtained with an FTIR spectrophotometer (Prestiger-21, Japan). The morphology and element information of the floc

Table 3
Details of algae solution in flocculation experiments[a]

Index	bEOM	dEOM
Algae culture solution	+	+
Algae cells alone[b]	−	−
Algae cells with bEOM	+	−
Algae cells + bEOM[c]	+ (centrifuged)	−
Algae cells + dEOM[d]	−	+ (centrifuged)

[a]+: existent; −: non-existent.
[b]Algae cells alone solution was prepared by re-suspending the collected algae cells which were centrifuged at 10,000 g for 15 min in the same volume of 0.6% NaCl solution.
[c]Algae cells + bEOM solution was prepared by re-suspending the collected algae cells which were centrifuged at 10,000 g for 15 min in the same volume of bEOM solution.
[d]Algae cells + dEOM solution was prepared by re-suspending the collected algae cells which were centrifuged at 10,000 g for 15 min in the same volume of dEOM solution.

Table 2
Basic water quality parameters of the bEOM and dEOM solutions extracted from *Microcystis aeruginosa* medium (cell number 1.03 × 10^9/L). Values represent mean ($n \geq 3$)

Sample	bEOM	dEOM
DOC (mg L^{-1})	12.22 (11.88–12.51)	30.20 (28.91–32.04)
Protein (mg L^{-1})	13.41 (12.08–14.44)	25.50 (23.92–27.14)
Polysaccharide (mg L^{-1})	9.76 (8.14–11.01)	28.77 (26.87–30.54)
SUVA (m^{-1} mg^{-1} L)	0.915	1.14
Zeta potential (mV)	−13.96 (13.48–14.26)	−21.65 (19.84–22.91)
Protein/DOC (mg/mg)	1.10	0.84
Polysaccharide/DOC (mg/mg)	0.80	0.95

sample were observed and detected with a scanning electron microscope (SEM, Tescan LMU, Czech Republic).

3. Results and discussions

3.1. Optimization of coagulation condition

3.1.1. Effect of dosage

Coagulant, dosage, and pH are the three crucial factors affecting the removal efficiency of bEOM and dEOM. To obtain the suitable coagulant and optimal dosage in coagulating bEOM and dEOM, various jar tests were performed using three coagulants (PFS, PDMDAAC, and PFS-PD) at different dosages. The pH of bEOM and dEOM solutions were adjusted to 8.0 ± 0.1 before the experiments. Fig. 1 plots the residual DOC and SUVA of bEOM and dEOM as a function of coagulant dosage. The DOC of bEOM and dEOM in Figs. 1a and b first decreased and increased, the optimum removal efficiency for bEOM was achieved by PFS-PD at 20 mg/L, and the optimum for dEOM was obtained by PFS-PD at 32 mg/L. PFS-PD showed the best efficiency among the three coagulants, whereas PDMDAAC was the least effective in the full flocculation dosage window. Inorganic coagulant PFS hydrolyzed into hydroxyl iron colloids after being dosed in the solution and can adsorb, sweep, and maintain complexity with abundant organic matters [21]. However, the poor settleability of PFS microflocs reduced its coagulation efficiency. PDMDAAC facilitated the bridging of macromolecule organics and microflocs to form large flocs through its positively charged extended loops and settlement [22,23]. The coagulation efficiency for the micromolecule organics was poor because of the linear molecular structure of PDMDAAC. Composite coagulant PFS-PD possessed the merits of PFS and PD. Thus, the negatively charged medium and organic matters micromolecule were adsorbed on insoluble hydroxides to form microflocs with the administration of PFS-PD [22]. Meanwhile, PDMDAAC absorbed the negatively charged

macromolecule organic matters and suspended microflocs, grew into large flocs, and precipitated. The mechanisms will be investigated in detail in the following section.

Moreover, the curve showed that the highest removal efficiencies for bEOM and dEOM by PFS-PD were 36.62% and 19.08%, respectively. The removal efficiencies for bEOM and dEOM by PFS and PD exhibited similar trends. The result indicated that the removal efficiency of dEOM through coagulation was less than that of bEOM, and the coagulation of dEOM was more difficult compared with that of bEOM. During the coagulation of bEOM and dEOM, the properties (e.g., constituent, MW distribution, and hydrophilicity) of organics significantly affected the coagulation behavior, leading to the difference in coagulation efficiency between bEOM and dEOM. The optimal coagulant for bEOM and dEOM removal was PFS-PD at dosages of 20 and 32 mg/L, respectively.

3.1.2. Effect of pH

The effect of the solution's initial pH on the coagulation efficiency of bEOM and dEOM by PFS-PD at pH 4–10 was analyzed. The results are displayed in Fig. 2. The plot in Fig. 2 indicated that the appropriate pH window of the three coagulants for bEOM and dEOM removal ranged from 6 to 9, and the colloidal solution was relatively stable at pH < 6 and >9. This result was attributed to the fact that organic matters can be absorbed, enmeshed, form flocs, and precipitated in the proper pH range (6–9) [24]. However, the charge repel effect that dominated in the acid (pH < 6, positively charged) and alkali solutions (pH < 6, positively charged) was adverse to the aggregation of colloids/particles and sedimentation of flocs [12]. pH 8.0 was adopted for the coagulation of bEOM and dEOM in this study. Notably, among the three coagulants, composite coagulant PFS-PD cleared more organic matters and achieved superior acid and alkali resistance in bEOM and dEOM coagulation.
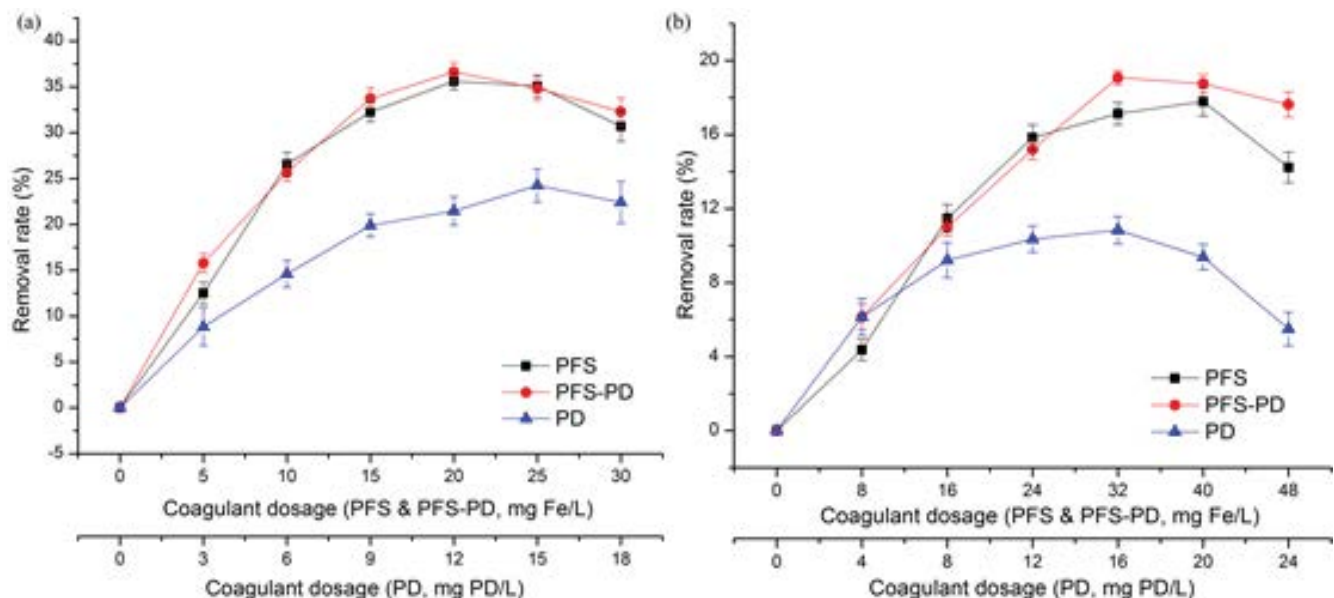

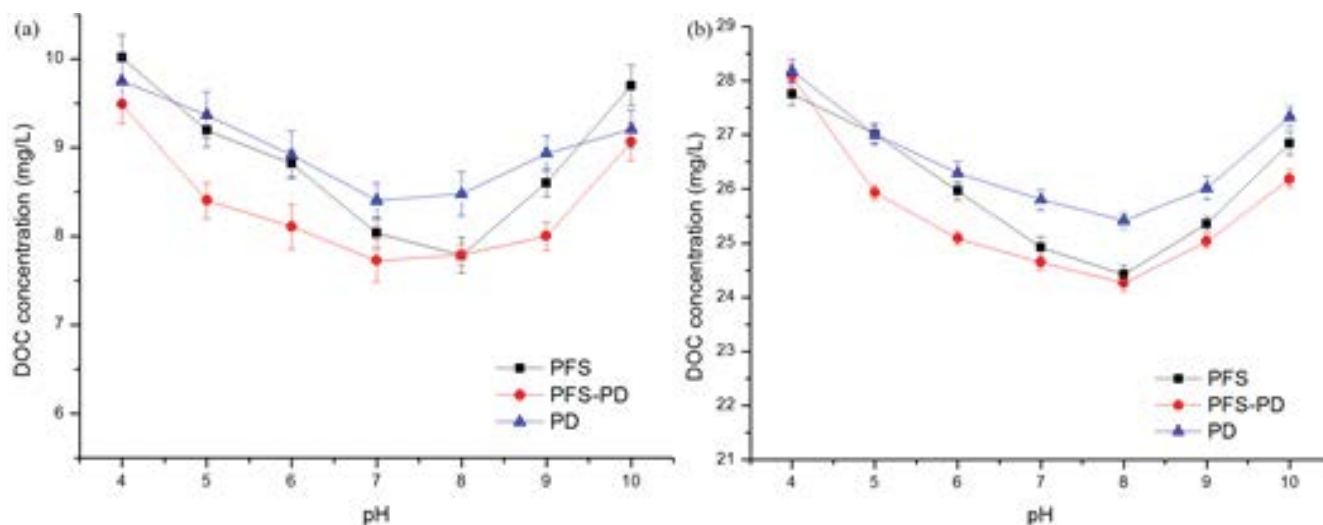Fig. 1. DOC removal rates of (a) bEOM and (b) dEOM in treated water with different coagulant dosage.

Fig. 2. Residual DOC of (a) bEOM and (b) dEOM in treated water with different initial pH.

3.2. Analysis of coagulation performance

From the above coagulation analysis, pH 8.0 and dosages of 20 and 32 mg/L of the composite coagulant PFS-PD for bEOM and dEOM, respectively, were adopted in the following experiments. Different from numerous studies that reported the removal efficiency of algae EOM through coagulation, the present study focused on the impact of EOM characteristics on coagulation behavior, especially on facilitating or weakening the coagulation efficiency [9,25]. Thus, the variations of SUVA, MW distribution, and fluorescent properties of organics during coagulation were evaluated through DOC/UV$_{254}$, UF fractionation, and 3D-EEM fluorescence spectrum, respectively, to better understand the coagulation of bEOM and dEOM.

The data in Table 2 show that the SUVA value of bEOM was lower than that of dEOM, indicating that the main compounds of bEOM had relatively lower content of unsaturated C–C bonds than do the main compounds of dEOM. The unsaturated organics in EOM frequently covered lipid, hydrocarbons, and humic-like substances, whereas few unsaturated bond structures were discovered in protein, polypeptide, and saccharide-like compounds [4,26]. The results suggested that the content of protein/polypeptide constituents in bEOM was more than that in dEOM, whereas the humic-like constituents presented opposite result [8,17], which correlate well with the value of protein/DOC and polysaccharide/DOC in Table 2. The trend of SUVA variation reflected the change of compositions [8]. Fig. 3 shows that the SUVA of bEOM remains constant during flocculation, while the SUVA of dEOM increases a point, indicating that many unsaturated C–C bonds are retained in the treated dEOM solution. The content of aromatic-like substances in dEOM increased after coagulation. The high amount of aromatic-like compounds may increase the risk of trihalomethane (disinfection by-products) formation during chlorination [25].

A comparison of the removal efficiency of DOC, proteins, and polysaccharides of bEOM and dEOM revealed that the removal efficiency of bEOM is higher than that of dEOM, whose proteins are the most evident in Table 4.
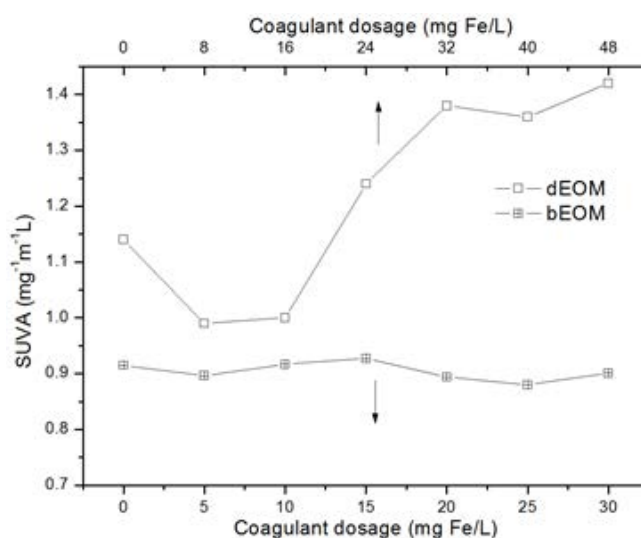

Fig. 3. SUVA values of (a) bEOM and (b) dEOM in the treated water with the different coagulant dosage.

The data illustrated that the removal rate of bEOM constituents reached more than 36% (exceeding 40% for proteins), whereas the removal of dEOM constituents was only 20%. The removal of dEOM was more difficult than that of bEOM, a discrepancy that may be related to the property difference between bEOM and dEOM in terms of constituents, MW distribution, and hydrophilicity [27,28]. UF fractionation and 3D-EEM fluorescence spectrum were applied to determine the change in MW distribution and fluorescent properties of organic fractions during coagulation for a precise interpretation of the above results.

In this study, the changes in MW distribution before (BC) and after (AC) coagulation were analyzed. The proportion of DOC, proteins, and polysaccharides at MWs of <1, 1–10, 10–30, 30–100, and >100 kDa fractions are depicted in Fig. 4. In terms of the DOC of bEOM, organics with MWs higher than 100 kDa comprised the dominant fractions (45.11%) followed

Table 4
Concentration of DOC, proteins and polysaccharides of (a) bEOM and (b) dEOM before and after coagulation process

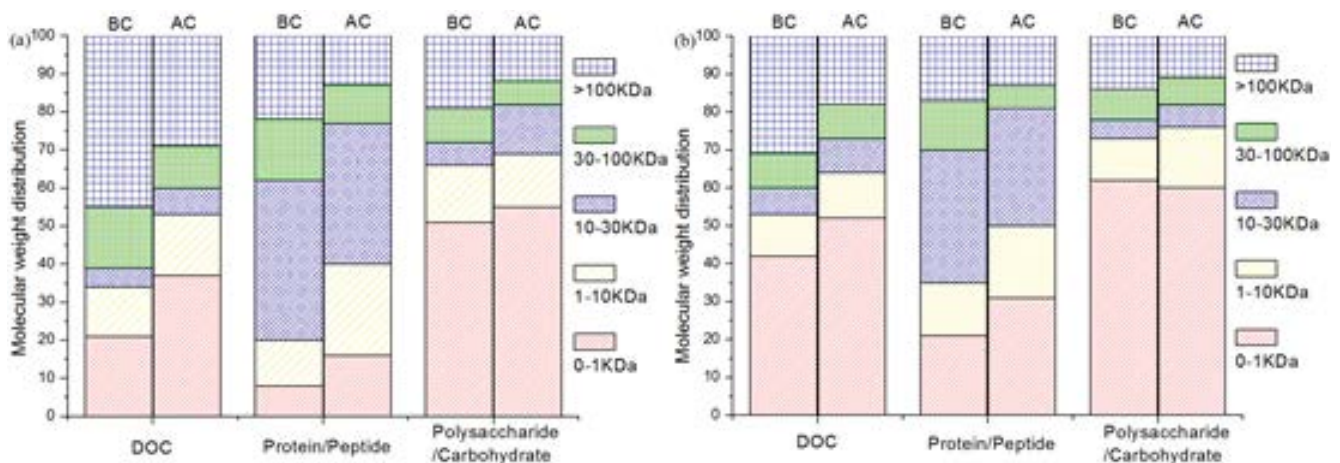| Sample		Before coagulation (mg L^{-1})	After coagulation (mg L^{-1})	Removal rate (%)
DOC	bEOM	12.22 (11.88–12.51)	7.75 (7.07–7.96)	36.62
	dEOM	30.20 (28.91–32.04)	24.44 (23.84.88–25.01)	19.08
Protein	bEOM	13.41 (12.08–14.44)	7.91 (7.58–7.95)	40.79
	dEOM	25.50 (23.92–27.14)	21.30 (20.66–21.51)	16.50
Polysaccharide	bEOM	9.76 (8.14–11.01)	6.73 (6.46–7.81)	31.00
	dEOM	28.77 (26.87–30.54)	21.10 (20.10–21.51)	23.20

Fig. 4. Molecular weight distribution of DOC, proteins and polysaccharides of (a) bEOM and (b) dEOM before and after coagulation process.

by those in 0–1 kDa. After coagulation, the largest portion was occupied by the compounds at 0–1 kDa (36.80%), followed by those larger than 100 kDa. Compared with bEOM, dEOM with a MW of 0–1 kDa fraction comprised a large proportion, which slightly increased after coagulation. Previous literature showed that the release of cellular organic matter (COM) is the source of bEOM [25,29], and the dominant constituents include polysaccharide-like fraction (e.g., starch in the form of amylose and amylopectin, peptidoglycans) and peptide/protein-like compounds (e.g., structural proteins, extracellular enzymes) [8,17,30]. Figs. 4a and b indicate that protein-like compounds with MWs of 10–30 kDa form the highest portion of bEOM (36.85%) and dEOM (34.82%). Similar to DOC, an increasing trend was observed between bEOM and dEOM, where protein-like substances with MWs lower than 10 kDa (0–1 and 1–10 kDa) fraction, and the portion >10 kDa decreased after coagulation. For polysaccharides, the components with low-MW (0–1 kDa) comprised the vast majority in bEOM and dEOM, with the amount in dEOM higher than that in bEOM. Coagulation decreased the proportion of macromolecule (>100 kDa) fraction, and no outstanding change was observed in other portions.

During the metabolism of *M. aeruginosa*, many COM components, such as peptide/protein, peptidoglycans, and polysaccharides, were released outside the cell walls. Thus, the new bEOM was characterized with a long chain and high-MW, where most of the functional groups on the molecules were charged through polarization [7,31]. High-MW

fractions, such as peptidoglycan, glycoprotein, and exoenzyme-like substances released from the cell walls, cross-linked together and formed a cohesive gelatinous substance [7,32]. The EOM bounded on cytoderm was centrifuged and suspended. The hydrolyzed $Fe_n(OH)_m^{(3n-m)+}$ (am) compounds absorbed and coagulated the majority of high-MW hydrophobic grouping fractions, and bEOM was coagulated [33]. Meanwhile, the released bEOM constantly accumulated, and exothecium compounds were desquamated and suspended in the cultivation media. The heterotrophic microorganisms in *M. aeruginosa* solution degraded macromolecular organics into micromolecular organics [27]. Thus, peptide/proteins and peptidoglycans/polysaccharides were partially degraded by the heterotrophic bacteria or associated exoenzyme, and numerous resolvable low-MW organics (e.g., aldehydes, carboxylic acids, hydrocarbons, oligosaccharides) were renamed as dEOM [27,34]. This outcome is the explanation for the differences in DOC, proteins, and polysaccharide properties of bEOM and dEOM and is the primary reason leading to the difference in removal efficiencies of bEOM and dEOM.

Fig. 5 illustrates the recorded 3D fluorescence spectra of bEOM and dEOM before and after coagulation. The dominated EEM fluorescence spectrum of bEOM contained peaks T_1 (Em305–350 nm/Ex270–280 nm), T_2 (Em300–349 nm/Ex220–260 nm), and C (Em420–460 nm/Ex250–280 nm), while the dominated spectrum of dEOM contained T_1, C, and S (Em370–420 nm/Ex310–340 nm) peaks according to fluorescence regional integration (FRI) of Chu and Chen [8,35]. The
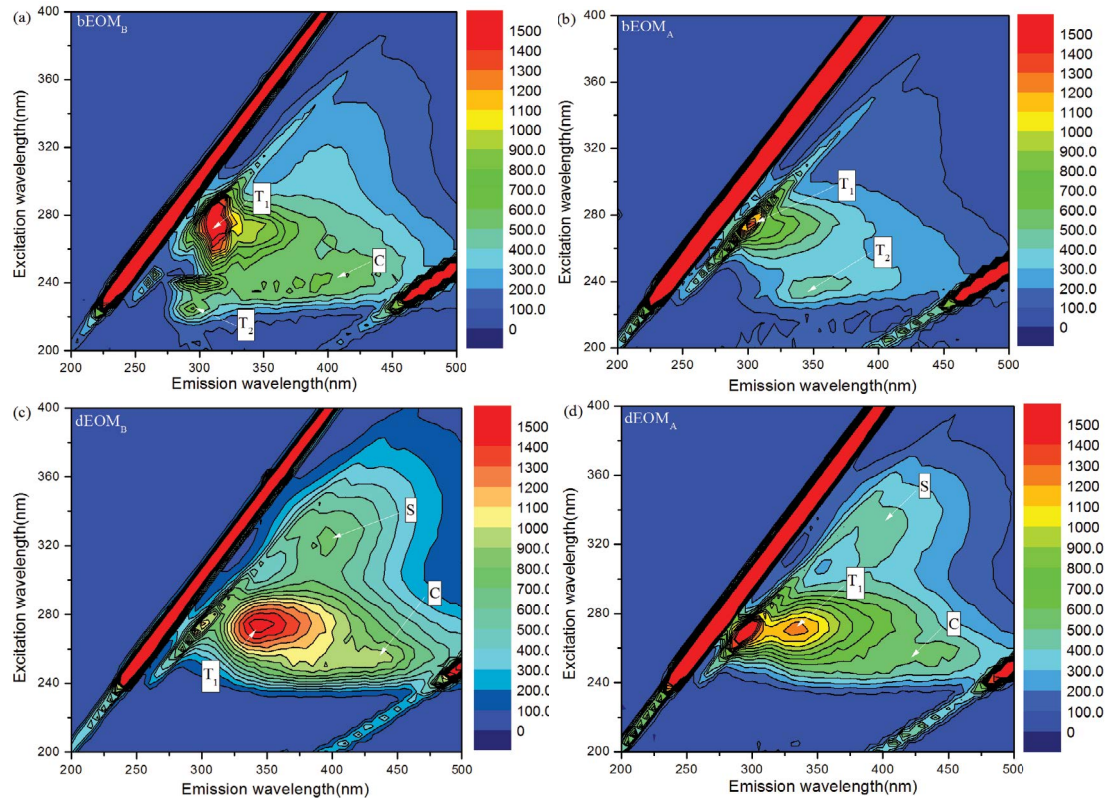
Fig. 5. Fluorescence EEM spectra of (a) bEOM, (b) bEOM after coagulation, (c) dEOM and (d) dEOM after coagulation.

prominently strong peak T_1 was related to protein-like (tryptophan) substances [9,36], and the intensity of fluorescence responses in bEOM was stronger than that of dEOM. This finding indicated that the content of protein-like compounds per unit DOC concentration in bEOM was higher than that in dEOM, consistent with the results in Table 2. Compared with the intensity of fluorescence responses during coagulation, a substantial decrease of fluorescence responses in the T_1 region was observed in bEOM after coagulation, whereas a slight reduction was observed in dEOM. This condition was attributed to the high-MW protein-like fraction of bEOM being easier to clear compared with that of dEOM during coagulation. Peak T_2 in Fig. 5a represents an aromatic protein-like substance that is associated with the existence of tryptophan-like substances and is absent in dEOM [37]. Peaks C and S in Figs. 5c and d are associated with humic-like and soluble microbial product-like substances, respectively [8,15]. The occurrence of large amounts of humic-like substances in dEOM was caused by the degradation of protein-like substances through biological activity [8,38]. No remarkable decrease in fluorescence intensity was observed after coagulation, indicating that microbial product-like and fulvic/humic-like substances are the toughest organics to remove through coagulation [9].

3.3. Interaction of bEOM/dEOM and coagulant

The characteristics of EOM affect the coagulation behavior of coagulants. To achieve an in-depth understanding of the reaction and interaction of EOM and coagulants, the flocs of bEOM and dEOM after coagulation were collected and samples were prepared. The functional groups, surface morphology, and element information of flocs were obtained through FTIR, SEM, and energy disperse spectroscopy (EDS) analysis. Given that inorganic salt occupied the majority of the EOM solution and a small amount of EOM cannot be separated effectively, only the flocs of EOM were investigated in this study.

Fig. 6 illustrates the FTIR of bEOM and dEOM flocs, where coagulants PFS and PDMDAAC were used as reference to identify the changes in their composition and functional groups. A wide and strong band between 3,450 and 3,423 cm^{-1} was observed in four samples; this band was assigned to the O–H and N–H stretching vibration of organic compounds, coupled with the O–H stretching vibration of hydroxyl iron in the curve of bEOM and dEOM flocs [26,39]. Similarly, the absorption peak around 1,634 cm^{-1} in curves a and b corresponded to the bending vibration of absorbed and crystallized H–O–H, and the absorption peak around 1,532 cm^{-1} in c and d was attributed to the amide I (C–O/C–N stretching vibration) from proteins and polysaccharides. Compared with a, the strong adsorption peaks at 1,134 and 1,127 cm^{-1} (SO_4^{2-} symmetrical and antisymmetrical stretching vibrations, respectively) and at 599 cm^{-1} (stretching vibrations of Fe–O bonds) in curves c and d covered, weakened, and disappeared, indicating that the organics adsorbed and interacted with hydroxyl iron and changed into the moderate peak [9,40]. Many organic groups were observed in bEOM flocs and disappeared in dEOM flocs. The adsorption bonds at 2,427; 1,383; and 836 cm^{-1} corresponding to the P–H

stretching vibration of proteins, C–H symmetric transformation vibration of polysaccharides, and C–H bending vibration of organic substances of bEOM flocs, respectively, were evaluated [8,19,41]. The results can be attributed to the fact that, in addition to reacting with hydroxyl iron, a large number of macromolecular organics of bEOM twined on the surface of flocs and were detected by infrared spectroscopy. By contrast, complex complexation occurred between the micromolecules of dEOM and hydroxyl iron, and few groups were in the unbound state and could not be observed by FTIR spectra. The above assumption was verified by Jia and Tang [9,42].

The flocs were investigated through surface morphology (SEM) and element information (EDS), and the results are exhibited in Fig. 7. The morphology of bEOM flocs was irregular with dense small protuberances on the surface and a compact structure. The irregular upheaval appearance was caused by the twisting or rolling of high-MW organic substances and particles, which formed a compact structure [8]. dEOM flocs showed a blocky structure with many irregular lamellar and granulum on the surface. The granulate and compact floc structure was caused by the high-MW polypeptide/protein or starch/polysaccharide-like substances that chelated and absorbed on the surface of the hydroxyl iron compound and the irregular morphology formed during floc sample preparation [43,44]. EDS analysis results showed that the major elements in the two flocs were C, N, O, Na, and Fe. Fe originated from the coagulant after coagulation. The element content was closely related to the organics species, and nitrogen, phosphorus, and sulfur were the main elements in polypeptide/protein-like substances. The ratio of (N+P+S) to C in bEOM flocs (1.35) was higher than that in dEOM (0.74), suggesting that more protein-like substances were coagulated and precipitated during bEOM treatment.
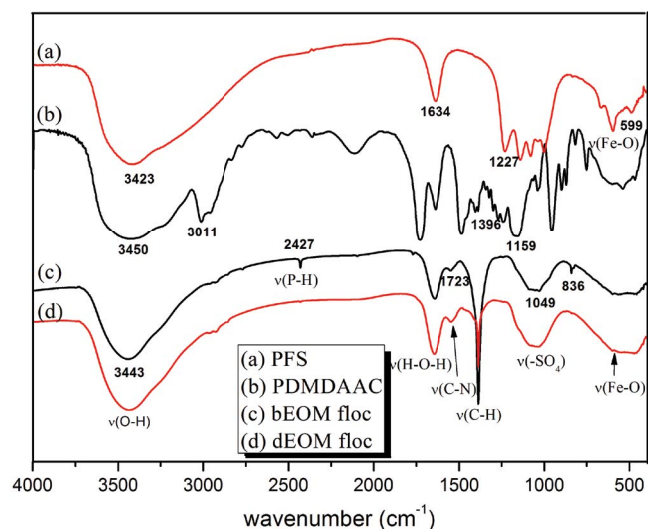

Fig. 6. FT-IR spectra of (a) PFS, (b) PDMDAAC, (c) bEOM flocs and (d) dEOM flocs.
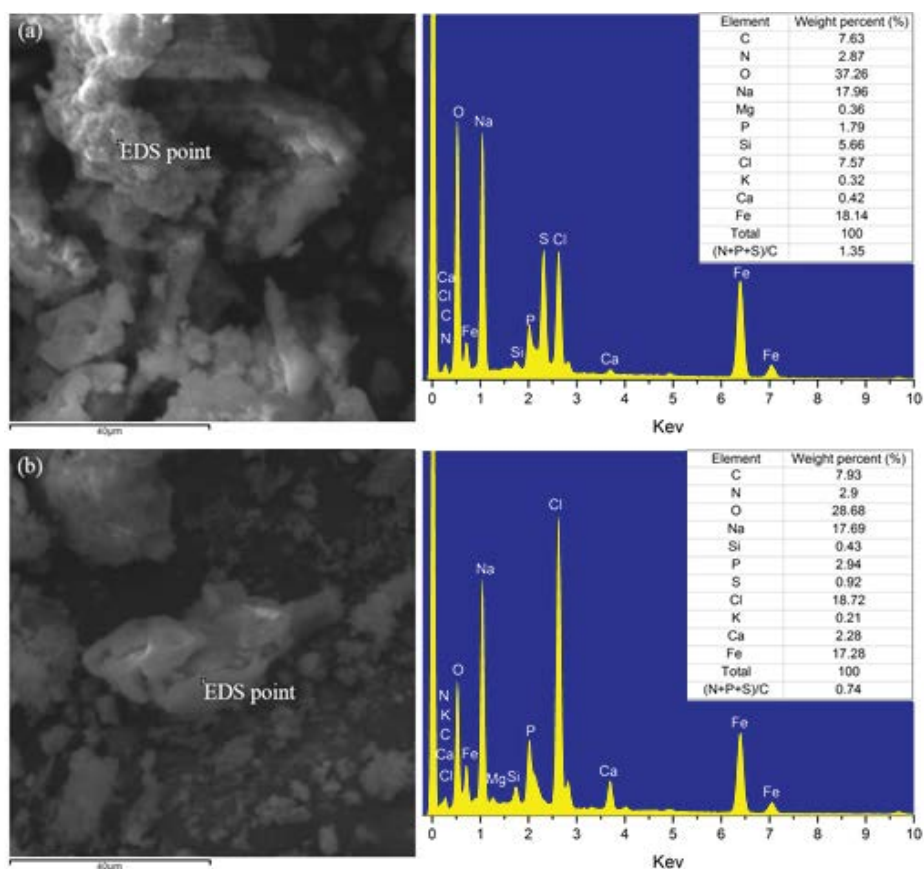

Fig. 7. SEM and EDS information of (a) bEOM and (b) dEOM flocs.

3.4. Investigation of the coagulation mechanism

The mechanism during bEOM and dEOM coagulation should be investigated and determined to improve the removal efficiency of organics. Fig. 8 displays the zeta potential response of bEOM and dEOM colloidal solutions as a function of PFS, PFS-PD, and PDMDAAC dosages. The zeta potential of dEOM (−21.65 mv) was higher than that of bEOM (−13.96 mv) before coagulation, and the zeta potential of two water samples decreased with the addition of a coagulant. The isoelectric point was achieved at the dosage range of 20–30 and 35–55 mg/L for bEOM and dEOM, respectively. Generally, the dominant mechanisms involved in coagulation are charge neutralization, adsorption bridging, and sweeping flocculation [45]. Given the impurity removal in Fig. 1, where the organic removal efficiency rose along with the increase in dosage, the superior efficiency appeared in the ranges of 20–25 and 32–40 mg/L for bEOM and dEOM,
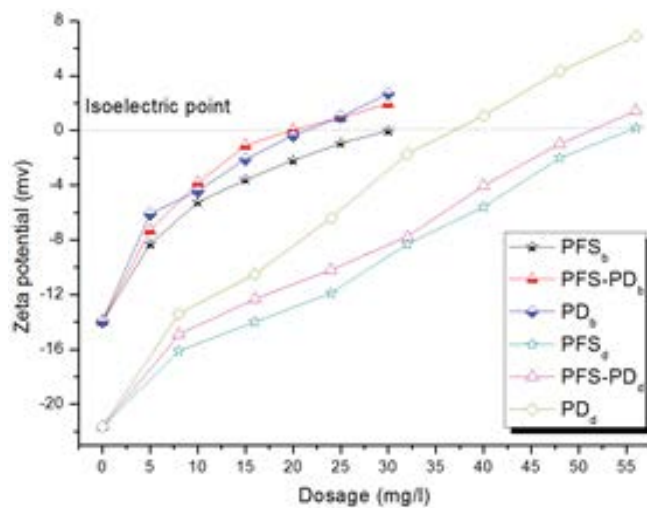
respectively. The similar dosage range between the highest organic removal and the isoelectric point indicated that charge neutralization plays an essential role in coagulation [9,23]. However, the zeta potential in Fig. 8 indicated that PDMDAAC exhibited the strongest charge neutrality ability; whereas the organic matters removal in Fig. 1 was the worst. Composite PFS-PD exhibited better coagulation efficiency than that by PDMDAAC. The results suggested that the charge neutrality mechanism is not the only role involved in coagulation [8,9].

In this study, the floc size distributions of bEOM and dEOM coagulated by PFS, PFS-PD, and PDMDAAC were evaluated to determine the coagulation mechanism. Fig. 9 shows the floc size distributions of bEOM and dEOM under coagulants PFS, PFS-PD, and PDMDAAC, and the d_{10}, d_{50}, and d_{90} floc sizes are displayed in Table 5. Floc size largely depends on the MW of the coagulant/flocculant and impurity colloid size and concentration [23]. A comparison of the floc size coagulated by three coagulants revealed that flocs with PDMDAAC was the maximum, followed by PFS-PD and PFS. In addition, the floc size of bEOM was larger than that of dEOM under PFS, PFS-PD, and PDMDAAC. The results were attributed to the superior bridging and trapping effect of the linear polymer flocculant PDMDAAC or the macromolecular composition in bEOM. Moreover, many fine aggregates

Fig. 8. Zeta potential of bEOM and dEOM solution after dosing three coagulants after coagulation.

Table 5
d_{10}, d_{50} and d_{90} for (a) bEOM and (b) dEOM by dosing three coagulants

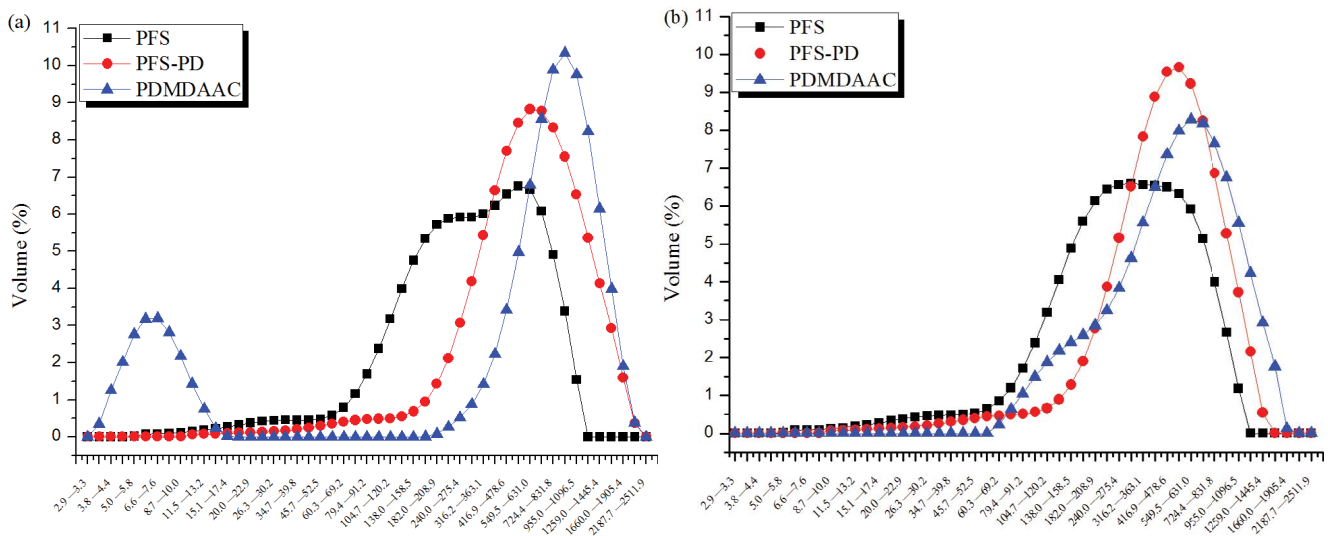| Sample		d_{10} (μm)	d_{50} (μm)	d_{90} (μm)
bEOM	PFS	98.223	302.612	721.541
	PFS-PD	238.211	588.909	1,224.556
	PDMDAAC	6.729	731.53	1,322.194
dEOM	PFS	95.633	283.86	681.628
	PFS-PD	185.236	450.313	866.263
	PDMDAAC	159.327	508.923	1,068.464

Fig. 9. Floc size distribution of (a) bEOM and (b) dEOM by dosing three coagulants after coagulation.

of microflocs were cross-linked through the bridging and sweeping effect to form large net-like flocs during coagulation. Thus, the bridging mechanisms induced by polymer macromolecules are significant to floc growth. As illustrated in Fig. 1, the DOC removal efficiency of PDMDAAC was the worst, indicating that no direct connection existed between the bridging effect induced by coagulant and organic removal. Meanwhile, the removal efficiency of bEOM was higher than that of dEOM, suggesting that the bridging effect induced by organics contributed to their removal.

FTIR analysis results manifested that hydroxyl iron can coordinate with C–N and N–H groups. The organics chelated with hydroxyl iron colloids may facilitate the adsorption of organic substances on hydroxyl iron or occupy the adsorption site and impede the coagulation. In terms of bEOM, many hydrophobic macro organics were adsorbed on the surfaces of $Fe_n(OH)_m^{(3n-m)+}$ (am) and formed primary microflocs through adsorption neutralization. The high-MW organics cross-linked with primary microflocs and became flocs and precipitated. The low removal efficiency corresponding to the slow decrease of zeta potential in dEOM treatment was caused by the amount of peptide/protein fragments in micromolecule organic matter, which might chelate with hydroxyl iron and be adsorbed on the surfaces of Fe_n and $Fe_n(OH)_m^{(3n-m)+}$ (am). The effective adsorption sites were occupied and charge reversal was not obvious in dEOM coagulation, ultimately resulting in the impediment of coagulation. Thus, in addition to charge neutralization and adsorption bridging action, chemical complexation mechanisms significantly influenced the coagulation efficiency, the deviation between superior coagulant and dosage obtained the highest efficiency, and the isoelectric point and floc size could be well explained by chemical complexation mechanisms during coagulation process.

When floc size, zeta potential, and organic removal are considered, it can be deduced that, in addition to charge neutrality and bridging mechanism, the complexing action between organic matters and hydroxyl colloid $Fe_n(OH)_m^{(3n-m)+}$ (am) is equally significant. The coagulation could be described where hydroxyl colloids and dendritic bodies were formed with coagulant administration, and the linear organic macromolecule matter absorbed and enmeshed on the coagulant and formed primary microflocs [44]. The primary microflocs were trapped and grew through the absorption and bridge effect by cationic polymeric flocculant PDMDAAC, resulting in the superior removal efficiency and large particle size of coagulant PFS-PD. The above coagulation theoretical research can provide another perspective to improve coagulation efficiency in practical applications.

After the coagulation behavior of bEOM and dEOM were investigated, the roles of bEOM and dEOM on the harvest of algae cells with PFS-PD were evaluated in terms of Chl-a removal. The results are displayed in Fig. 10. An acceptable performance with removal rates over 90% was observed at the dosage range of 30–45 mg/L. In terms of the dosage demand that could achieve the highest removal efficiency, algae cells alone and algae cells with bEOM were least (15–20 mg/L), and the dosage for algae cells + dEOM and algae culture solution was unacceptable (>30 mg/L). bEOM was released to the surface incessantly because the algae cells
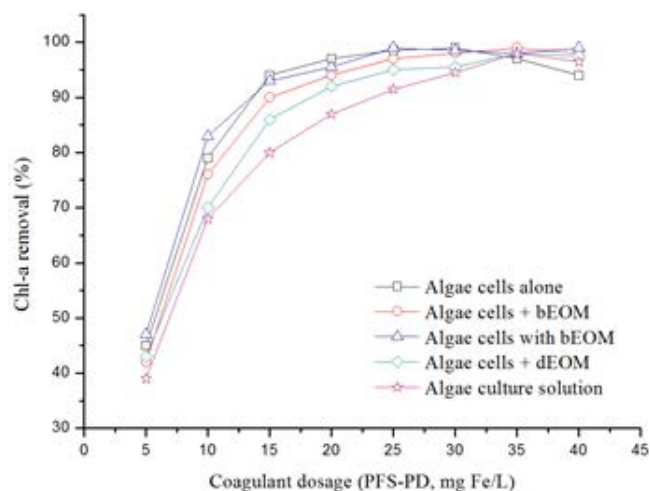

Fig. 10. Changes of Chl-a removal with different EOM and coagulant dosage.

used in experiments remained active, and the difference between algae cells alone and algae cells with bEOM was negligible. The adhering bEOM showed a positive impact on algae removal, followed by the dissociative bEOM, and the dEOM in the solution remarkably impeded the coagulation efficiency. The result confirmed that bEOM with high-MW and protein-like substance presents strong complexation and interactions with hydroxyl iron. The complexation and interactions between bEOM and $Fe_n(OH)_m^{(3n-m)+}$ (am) and the entrapment of bEOM and PDMDAAC with formed flocs contribute to the removal of algae cells and bEOM, especially when the bEOM adheres to the surface of cells. By contrast, the low-MW dEOM chelates with hydroxyl iron and adsorbs on the surface of hydrocolloids. Given that the charge reversal is not obvious in dEOM treatment, dEOM performs an obstructive role and impedes the coagulation; specifically, the more dEOM in the solutions, the lower the removal efficiency.

4. Conclusions

Coagulant PFS-PD showed superior coagulation efficiency in the removal of bEOM and dEOM compared with PFS and PDMDAAC. An acceptable performance of bEOM removal was observed in terms of high removal rate of protein- and polysaccharide-like substances and DOC. The interactions of function groups N–H, C–N, and C–O of high-MW bEOM with hydroxyl iron promoted the adsorption–bridging effect of organic matters, coagulant, and algae cells. The chemical chelation function of low-MW dEOM with hydroxyl iron decreased the adsorption capacity of $Fe_n(OH)_m^{(3n-m)+}$ and lowered the coagulation efficiency, resulting in a large demand of coagulant dosage and low efficiency of algae harvest. This study provides an important reference for algae-laden water treatment projects.

Abbreviations

MW	—	Molecular weight
PFS	—	Polyferric sulfate
DOC	—	dissolved organic carbon

PDMDAAC (PD)	—	Polydimethyl diallyl ammonium chloride
dEOM	—	Dissolved extracellular organic matter
bEOM	—	Bounded extracellular organic matter
SUVA	—	Specific ultraviolet absorbance
3D-EEM	—	Three dimensional Excitation emission spectra
Chl-a	—	Chlorophyll-a
BC	—	Before coagulation
AC	—	After coagulation

Acknowledgments

References

[1] J. Sun, L. Bu, L. Deng, Z. Shi, S. Zhou, Removal of *Microcystis aeruginosa* by UV/chlorine process: Inactivation mechanism and microcystins degradation, Chem. Eng. J., 349 (2018) 408–415.

[2] Z. Yu, H. Pei, Q. Hou, C. Nie, L. Zhang, Z. Yang, X. Wang, The effects of algal extracellular substances on algal growth, metabolism and long-term medium recycle, and inhibition alleviation through ultrasonication, Bioresour. Technol., 267 (2018) 192–200.

[3] F. Zhao, Y. Su, X. Tan, H. Chu, Y. Zhang, L. Yang, X. Zhou, Effect of temperature on extracellular organic matter (EOM) of *Chlorella pyrenoidosa* and effect of EOM on irreversible membrane fouling, Colloids Surf., B, 136 (2015) 431–439.

[4] F. Qu, H. Liang, J. He, J. Ma, Z. Wang, H. Yu, G. Li, Characterization of dissolved extracellular organic matter (dEOM) and bound extracellular organic matter (bEOM) of *Microcystis aeruginosa* and their impacts on UF membrane fouling, Water Res., 46 (2012) 2881–2890.

[5] J. Chen, N. Gao, L. Li, M. Zhu, J. Yang, X. Lu, Y. Zhang, Disinfection by-product formation during chlor(am)ination of algal organic matters (AOM) extracted from *Microcystis aeruginosa*: effect of growth phases, AOM and bromide concentration, Environ. Sci. Pollut. Res., 24 (2017) 1–10.

[6] J. Xu, Y. Zhao, B. Gao, S. Han, Q. Zhao, X. Liu, The influence of algal organic matter produced by *Microcystis aeruginosa* on coagulation-ultrafiltration treatment of natural organic matter, Chemosphere, 196 (2018) 418–428.

[7] R.K. Henderson, A. Baker, S.A. Parsons, B. Jefferson, Characterisation of algogenic organic matter extracted from cyanobacteria, green algae and diatoms, Water Res., 42 (2008) 3435–3445.

[8] H. Chu, H. Yu, X. Tan, Y. Zhang, X. Zhou, L. Yang, D. Li, Extraction procedure optimization and the characteristics of dissolved extracellular organic matter (dEOM) and bound extracellular organic matter (bEOM) from *Chlorella pyrenoidosa*, Colloids Surf., B, 125 (2015) 238–246.

[9] X. Tang, H. Zheng, B. Gao, C. Zhao, B. Liu, W. Chen, J. Guo, Interactions of specific extracellular organic matter and polyaluminum chloride and their roles in the algae-polluted water treatment, J. Hazard. Mater., 332 (2017) 1–9.

[10] W. Huang, H. Chu, B. Dong, Understanding the fouling of algogenic organic matter in microfiltration using membrane–foulant interaction energy analysis: effects of organic hydrophobicity, Colloids Surf., B, 122 (2014) 447–456.

[11] S.M. Korotta-Gamage, A. Sathasivan, A review: potential and challenges of biologically activated carbon to remove natural organic matter in drinking water purification process, Chemosphere, 167 (2017) 120–138.

[12] G. Zhu, Q. Wang, J. Yin, Z. Li, P. Zhang, B. Ren, G. Fan, P. Wan, Toward a better understanding of coagulation for dissolved organic nitrogen using polymeric zinc-iron-phosphate coagulant, Water Res., 100 (2016) 201–210.

[13] G. Zhu, J. Liu, Y. Bian, Evaluation of cationic polyacrylamide-based hybrid coagulation for the removal of dissolved organic nitrogen, Environ. Sci. Pollut. Res., 25 (2018) 14447–14459.

[14] H. Wang, F. Qu, A. Ding, H. Liang, R. Jia, K. Li, L. Bai, H. Chang, G. Li, Combined effects of PAC adsorption and in situ chlorination on membrane fouling in a pilot-scale coagulation and ultrafiltration process, Chem. Eng. J., 283 (2016) 1374–1383.

[15] R.K. Henderson, S.A. Parsons, B. Jefferson, The impact of differing cell and algogenic organic matter (AOM) characteristics on the coagulation and flotation of algae, Water Res., 44 (2010) 3617–3624.

[16] S. Huo, Y. Chen, Y. Liu, Y. Zhu, G. Peng, R. Dong, Experiment on microalgae cultivation in BG11 nutrient solution adding biogas slurry, Trans. Chin. Soc. Agric. Eng., 28 (2012) 241–246.

[17] M. Pivokonsky, J. Safarikova, M. Baresova, L. Pivokonska, I. Kopecka, A comparison of the character of algal extracellular versus cellular organic matter produced by cyanobacterium, diatom and green alga, Water Res., 51 (2014) 37–46.

[18] Z.J. Zhang, W. Sun, L.I. Yong-Liang, C.F. Zhang, Determination of polysaccharide in Rhizoma Polygonatii by phenol-sulfuric acid and DNS methods, Chin. J. Exp. Traditional Med. Formulae, 18 (2012) 106–109.

[19] W. Chen, H. Zheng, J. Guo, F. Li, X. Tang, B. Liu, Y. Zhou, Preparation and characterization of a composite coagulant: polyferric titanium sulfate, Water Air Soil Pollut., 227 (2016) 79.

[20] X. Sun, M.Q. Wu, Q.G. Xing, X.D. Song, D.H. Zhao, Q.Q. Han, G.Z. Zhang, Spatio-temporal patterns of *Ulva prolifera* blooms and the corresponding influence on chlorophyll-a concentration in the Southern Yellow Sea, China, Sci. Total Environ., 640 (2018) 807–820.

[21] W. Chen, H. Zheng, J. Zhai, Y. Wang, W. Xue, X. Tang, Z. Zhang, Y. Sun, Characterization and coagulation-flocculation performance of a composite coagulant: poly-ferric-aluminum-silicate-sulfate, Desal. Wat. Treat., 56 (2015) 1776–1786.

[22] C. Sun, Q. Yue, B. Gao, B. Cao, R. Mu, Z. Zhang, Synthesis and floc properties of polymeric ferric aluminum chloride–polydimethyl diallylammonium chloride coagulant in coagulating humic acid–kaolin synthetic water, Chem. Eng. J., 185–186 (2012) 29–34.

[23] W. Chen, H. Zheng, Q. Guan, H. Teng, C. Zhao, C. Zhao, Fabricating a flocculant with controllable cationic microblock structure: characterization and sludge conditioning behavior evaluation, Ind. Eng. Chem. Res., 55 (2016) 2892–2902.

[24] C.S. Lee, J. Robinson, M.F. Chong, A review on application of flocculants in wastewater treatment, Process Saf. Environ. Prot., 92 (2014) 489–508.

[25] L. Li, N. Gao, Y. Deng, J. Yao, K. Zhang, Characterization of intracellular & extracellular algae organic matters (AOM) of *Microcystic aeruginosa* and formation of AOM-associated disinfection byproducts and odor & taste compounds, Water Res., 46 (2012) 1233–1240.

[26] F.J. Rodríguez, P. Schlenger, M. Garcíavalverde, Monitoring changes in the structure and properties of humic substances following ozonation using UV-Vis, FTIR and (1)H NMR techniques, Sci. Total Environ., 541 (2016) 623–637.

[27] Z. Wang, C.M. Hessler, Z. Xue, Y. Seo, The role of extracellular polymeric substances on the sorption of natural organic matter, Water Res., 46 (2012) 1052–1060.

[28] B. Chen, F. Li, N. Liu, F. Ge, H. Xiao, Y. Yang, Role of extracellular polymeric substances from *Chlorella vulgaris* in the removal of ammonium and orthophosphate under the stress of cadmium, Bioresour. Technol., 190 (2015) 299–306.

[29] K.D. Kearns, M.D. Hunter, Green algal extracellular products regulate antialgal toxin production in a cyanobacterium, Environ. Microbiol., 2 (2000) 291–297.

[30] L.O. Villacorte, Y. Ekowati, T.R. Neu, J.M. Kleijn, H. Winters, G. Amy, J.C. Schippers, M.D. Kennedy, Characterisation of algal organic matter produced by bloom-forming marine and freshwater algae, Water Res., 73 (2015) 216–230.

[31] S. Zhou, Y. Shao, N. Gao, Y. Deng, L. Li, J. Deng, C. Tan, Characterization of algal organic matters of *Microcystis aeruginosa*: biodegradability, DBP formation and membrane fouling potential, Water Res., 52 (2014) 199–207.

[32] B.Q. Liao, D.G. Allen, G.G. Leppard, I.G. Droppo, S.N. Liss, Interparticle interactions affecting the stability of sludge flocs, J. Colloid Interface Sci., 249 (2002) 372.

[33] F. Sun, H.-Y. Pei, W.-R. Hu, C.-X. Ma, The lysis of *Microcystis aeruginosa* in $AlCl_3$ coagulation and sedimentation processes, Chem. Eng. J., 193–194 (2012) 196–202.

[34] Z. Xue, V.R. Sendamangalam, C.L. Gruden, Y. Seo, Multiple roles of extracellular polymeric substances on resistance of biofilm and detached clusters, Environ. Sci. Technol., 46 (2012) 13212–13219.

[35] W. Chen, P. Westerhoff, J.A. Leenheer, K. Booksh, Fluorescence excitation-emission matrix regional integration to quantify spectra for dissolved organic matter, Environ. Sci. Technol., 37 (2003) 5701–5710.

[36] G. Zhu, Y. Bian, A.S. Hursthouse, P. Wan, K. Szymanska, J. Ma, X. Wang, Z. Zhao, Application of 3-D fluorescence: characterization of natural organic matter in natural water and water purification systems, J. Fluoresc., 27 (2017) 2069–2094.

[37] C. Ma, W. Hu, H. Pei, H. Xu, R. Pei, Enhancing integrated removal of *Microcystis aeruginosa* and adsorption of microcystins using chitosan-aluminum chloride combined coagulants: effect of chemical dosing orders and coagulation mechanisms, Colloids Surf., A, 490 (2016) 258–267.

[38] C. Liu, J. Wang, Z. Cao, W. Chen, H. Bi, Variation of dissolved organic nitrogen concentration during the ultrasonic pretreatment to *Microcystis aeruginosa*, Ultrason. Sonochem., 29 (2016) 236–243.

[39] W. Chen, H. Zheng, H. Teng, Y. Wang, Y. Zhang, C. Zhao, Y. Liao, Enhanced coagulation-flocculation performance of iron-based coagulants: effects of PO_4^{3-} and SiO_3^{2-} modifiers, PLoS One, 10 (2015), https://doi.org/10.1371/journal.pone.0137116.

[40] G. Zhu, H. Zheng, W. Chen, W. Fan, P. Zhang, T. Tshukudu, Preparation of a composite coagulant: polymeric aluminum ferric sulfate (PAFS) for wastewater treatment, Desalination, 285 (2012) 315–323.

[41] G.E. Douberly, A.M. Ricks, B.W. Ticknor, M.A. Duncan, The structure of protonated acetone and its dimer: infrared photodissociation spectroscopy from 800 to 4,000 cm^{-1}, Phys. Chem. Chem. Phys., 10 (2007) 77–79.

[42] S. Jia, Z. Yang, W. Yang, T. Zhang, S. Zhang, X. Yang, Y. Dong, J. Wu, Y. Wang, Removal of Cu(II) and tetracycline using an aromatic rings-functionalized chitosan-based flocculant: enhanced interaction between the flocculant and the antibiotic, Chem. Eng. J., 283 (2016) 495–503.

[43] Y. Xu, T. Chen, F. Cui, W. Shi, Effect of reused alum-humic-flocs on coagulation performance and floc characteristics formed by aluminum salt coagulants in humic-acid water, Chem. Eng. J., 287 (2016) 225–232.

[44] H. Rong, B. Gao, M. Dong, Y. Zhao, S. Sun, Yanwang, Q. Yue, Q. Li, Characterization of size, strength and structure of aluminum-polymer dual-coagulant flocs under different pH and hydraulic conditions, J. Hazard. Mater., 252–253 (2013) 330–337.

[45] L. You, L. Song, A. Wang, F. Lu, Q. Zhang, Fabrication of a cationic polysaccharide for high performance flocculation, Colloids Surf., A, 520 (2017) 841–849.